SOLUTION MINING RESEARCH INSTITUTE
679 Plank Road
Clifton Park, NY 12065, USA

Telephone: +1 518-579-6587
www.solutionmining.org

Technical Conference Paper

Tightness of salt caverns used for hydrogen storage

Pierre Bérest, LMS, Ecole Polytechnique, IEP, Palaiseau, France

Benoît Brouard, Brouard Consulting, Paris, France

Grégoire Hévin, Storengy, Bois-Colombes, France

Arnaud Réveillère, Geostock SAS, Rueil Malmaison, France

SMRI Spring 2021 Virtual Technical Conference
19-22 APRIL 2021

Solution Mining Research Institute Spring 2021 Virtual Technical Conference

19-22 APRIL 2021

Tightness of salt caverns used for hydrogen storage

Pierre Bérest[1], Benoît Brouard[2], Grégoire Hévin[3], Arnaud Réveillère[4]

[1]LMS, Ecole Polytechnique, IEP, Palaiseau, France

[2]Brouard Consulting, Paris, France

[3]Storengy, Bois-Colombes, France

[4]Geostock SAS, Rueil Malmaison, France

Abstract

Tightness is a fundamental requisite of any storage cavern. Tightness results from (Bérest and Brouard, 2003): properties of the rock mass, nature of the stored products, quality of the cementing job, pressure and pressure changes of the stored fluids, and well architecture (i.e., the *completion*, or the number and the lengths of the cemented casings).

Much information and experience are available from the 2000+ salt caverns used worldwide for hydrocarbon storage. Generally speaking, salt permeability is exceedingly small. Several incidents proved that breaches or conduits can be created between a cavern and a neighboring cavern, or between a cavern and the boundaries of the salt formation. The origin of most of these incidents is the presence of Anomalous Zones in the salt formation. *In-situ* tests proved that the overall cavern permeability experiences a significant increase when fluid pressure at cavern depth is larger than 80-85% of the geostatic pressure.

However, as in most pressure vessels, it is the “piping” (the access well) that most often is the weakest point. Several incidents are described in this paper. The origin of most of these incidents is the presence of a single casing between the stored product and the rock formation.

In this context, tightness tests are mandatory. It is suggested to test the wellbore after drilling and to test the cavern before commissioning. The Nitrogen Leak Test, a high-resolution measurement technique, has become a standard. It consists of filling the annular space with pressurized nitrogen, setting the gas-brine interface below the last casing shoe, and tracking this interface with a logging tool. The mass of gas is very small when compared to brine mass, and accurate measurement of gas-mass changes during the test is possible. It is suggested to test the well with nitrogen and hydrogen, successively, and to set the gas-brine interface at various depths to track the leaks originating from different parts of the well. A cost-effective method, based on the observation of wellhead pressures, is proposed.

Key words: Hydrogen Storage in Salt Caverns, Tightness tests in salt caverns, Tightness of underground storages

1. Lessons drawn from salt caverns in which a breach was detected

Examples of salt caverns that were breached.

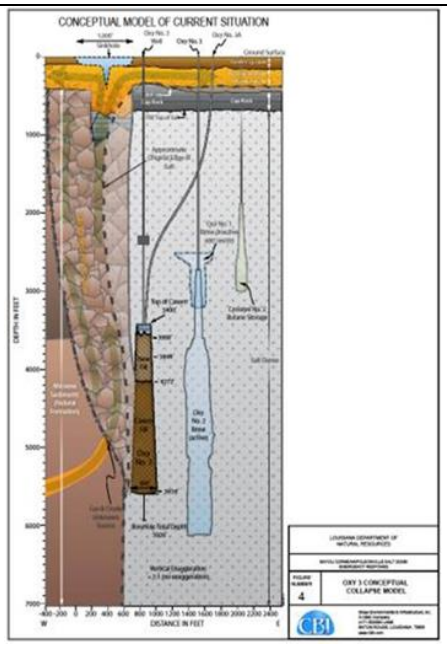

Figure 1a - Bayou Corne Oxy 3 conceptual model (CB&I).

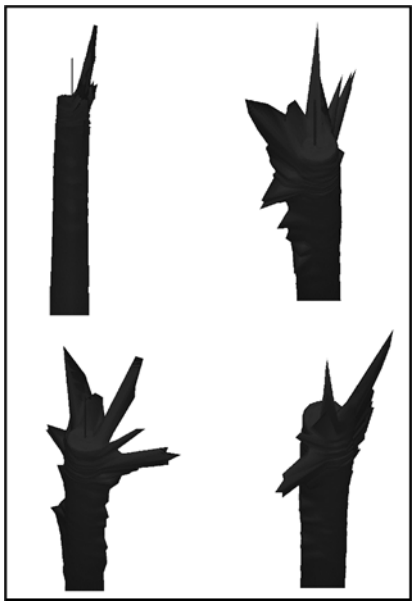

Figure 1b - Mont Belvieu Cavern 16E roof area (Cartwright and Ratigan, 2005).

Examples of salt caverns that were breached (continued).

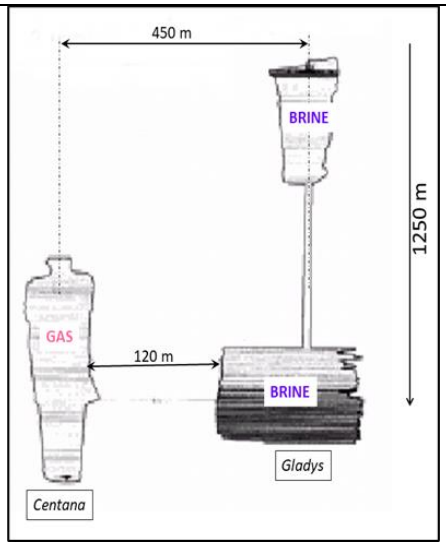

Figure 1c - Spindletop Centana 1 and Gladys 2 caverns (after Johnson, 2003).

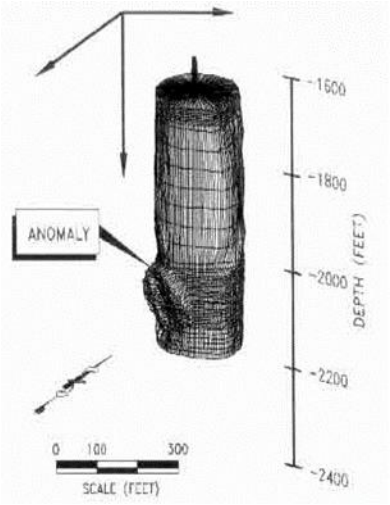

Figure 1d - Clovelly Salt Dome Cavern (McCauley et al., 1998).

Figure 1. Examples of salt caverns that were breached (concluded).

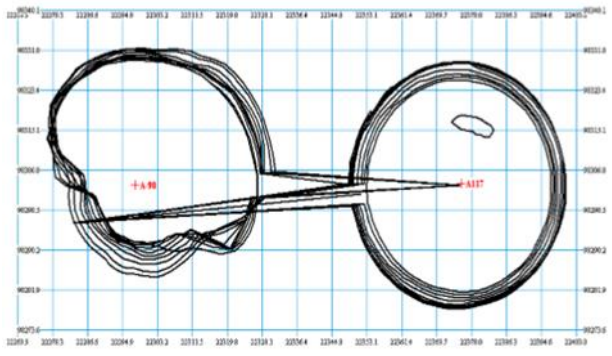

Figure 1e - Arabali Caverns a-98 and a-117 (Kirmic and Rałowicz, 2003).

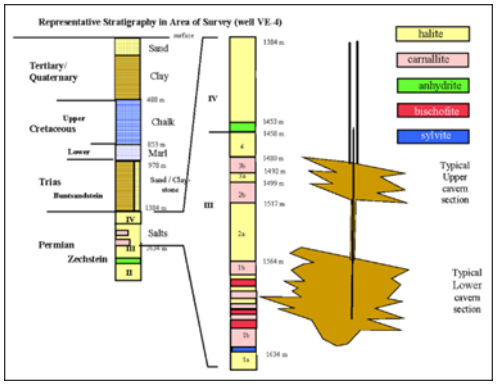

Figure 1f - Stratification of salts near Veendam, the Netherlands (Fokker et al., 2004).

Information on salt caverns used for brine production and hydrocarbon storage in which a breach was detected include some well-known cases. Information of these cases is provided in Figures 1(a-f), below, and summarized here. More details can be found in Réveilllère et al., 2017 (SMRI Report) and Bérest et al., 2018.

As illustrated in Figure 1a, a sinkhole was discovered in the swamp near Bayou Corne, Louisiana, on August 3, 2012. It quickly was suspected that the sinkhole was connected to Oxy3, a brine cavern located near the edge of the Napoleonville salt dome, whose roof and bottom were 3395 ft. (1050 m) and 5600 ft. (1700 m), respectively. Further investigation proved that loose and soft sediments flowed along the dome flank from ground level to a breach created in the lower part of the cavern where the salt wall was thin.

Regarding Figure 1b, a Mechanical Integrity Test (MIT) and pressure observations proved that Cavern 16E and neighboring Cavern 2E, two brine caverns in the Mont Belvieu, Texas, site were connected hydraulically; origin of the breach is likely to be an Anomalous Zone inside the dome

> (*"The term "anomalous features" (AFs) has been used by Kupfer (1990) to designate unusual features found in the stocks of Gulf Coast salt domes. Based on observations made in rock-salt mines, he identified ten major groups of AFs, including such items as intense structural folding, the presence of "impurities" (e.g., anhydrite, shales, and sandstones), gas releases, connate brine seeps, exceptionally large crystal size, potash, hydrocarbons, etc. He observed that these unusual features tended to cluster in linear trends through salt stocks; and, if they contained three or more AFs,* [he] *designated such trends as "anomalous zones (AZs)"* (Thoms and Neal, 1992, p. 1; see also Loof, 2017).

As seen in Figure 1c, gas originating from the Centana No. 1 natural-gas storage at Spindletop, Texas, leaked to the Gladys No. 2 brine cavern, although the distance between the two caverns is 120 m (400 ft.). Asymmetric growth and brine contamination by sylvite during an earlier enlargement of Centana No. 1 suggest the presence of an Anomalous Zone.

Clovelly salt dome Cavern No. 14, in Louisiana (see Figure 1d), an oil storage cavern, did not pass an MIT. This cavern is close to the side of the dome. Further investigation suggested that brine leaked to the exterior of the dome through a 660-m (2 200 ft.) deep "inhomogeneity".

In the Arabali brine field, Turkey (Figure 1e), a hydraulic connection was detected between Caverns a-98 and a-117. Sonar surveys suggested that a 9-m-high, 30-m-long, 2-m-wide (30 ft x 100 ft x 6 ft) slot was created between the two caverns, exactly coinciding with the vertical plane crossing through the hanging strings of each of the two caverns, a puzzling circumstance.

Regarding Figure 1f, at Veendam (the Netherlands), the mining method consists of selecting a rather high brine pressure (85% of geostatic) in the cavern to allow the Mg-salt to flow (squeeze) at a rate comparable to the solution-mining rate. (Over time, the cavern volume remains roughly constant.) On April 20, 2018, "*a sudden pressure drop occurred in the cluster* [a labyrinth composed of many roughly permeable conduits interconnecting nine caverns.] *Pressure dropped by about 2.5 MPa* [360 psi] *after 1 day and by about 3 MPa* [435 psi] *after 2 days, after which the situation stabilized"* (Smit, 2019, p. 2). The brine volume that seeped from the cluster during the first 30 minutes was estimated to be 25,000 m^3 (0.15 Mbbls). It has been hypothesized that the initial fracture or breach through the relatively thin salt layer (a dozen meters, or 40 ft.) at the top cluster opened in the overlying Bundsandstein layer, where the state of stresses is suspected to be strongly anisotropic, favoring swift fracture growth.

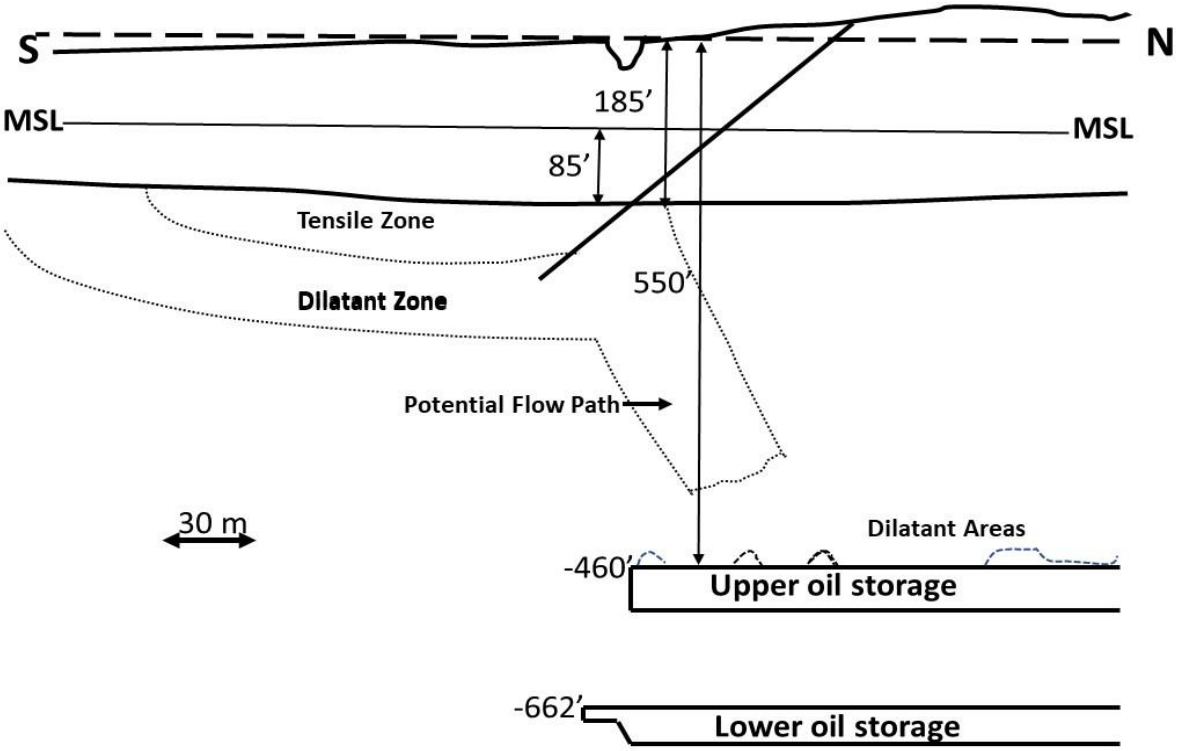

Figure 2 – Weeks Island Mine. [The mine was converted into an oil storage. Geomechanical modeling by Hoffman and Ehgartner (1997) showed mechanism for crack development in tension that would develop over mined openings after a number of years and progress through weakened dilatant zones (after Bauer et al., 2000).]

Somewhat related to this theme, the Weeks Island case is typical (Figure 2). This is a two-level room-and-pillar mine with the two levels, measured to the mine floor, 163-m (mined from 1902 to 1955) and 224-m (mined from 1955 to 1976) below the surface, respectively. The rooms height was 22 m to 23 m (72 ft. to 75 ft), the pillars were 30.5-m (100 ft.) wide, and the rooms were 15.2-m (50 ft.) wide, resulting in an extraction ratio of 55% (Bauer et al., 2000; Hoffman and Ehgartner,1996). Two sinkholes, the first one in 1992, appeared at ground level above the edge of the mine. Evidences suggested that brine was seeping to the mine, which was abandoned in 1995 (Bauer et al., 2000). Sinkhole creation was unexpected because the mine, which was stable during mining operations (Carosella, 1978), had been converted to an oil storage facility in 1981 and contained such (relatively) high fluid pressure in the mine that drastic mechanical evolutions (following conversion) did not seem likely. In fact, numerical computations (Bauer et al., 2000) suggest that the following sequence of events: creation of the mine – redistribution of stresses in the rock mass from 1902 to 1981 – increase of mine pressure resulting from filling with oil – new redistribution of stresses in the rock mass – may lead to the development of tensile stresses in the rock mass and formation of leak path crossing the salt formation from the mine to the edge of the dome. (Similar sequences are present in gas caverns and may explain cavern permeability increase when gas pressure is high, see Paragraph 3.1).

These examples prove that tightness can be lost when a cavern is too close to the salt formation boundaries or when a cavern intersects an Anomalous Zone, two circumstances that can be avoided when geological/geophysical investigations and tightness tests are performed.

2. Examples of caverns that experienced a loss of wellbore integrity

2.1. Factors contributing to wellbore integrity

Loss of access-well tightness in a dozen storage sites (to be compared to the 2000+ storage caverns operated worldwide) was described by Réveillère et al., 2017 (SMRI Report) and Bérest et al. (2018). Most of the leaks originated from the failure of a steel casing due to overstretching, shearing, corrosion, milling or fatigue, followed by permeation of the stored product through the cement sheath. In fact, well integrity results from several factors:

(a) properties of the rock mass,

(b) nature of the stored products,

(c) quality of the cementing job,

(d) pressure and pressure changes of the stored fluids, and

(e) well architecture (i.e., the *completion*, or the number and the lengths of the cemented casings).

Plastic rock formations, such as salt and clay, can have a very favorable effect in that they naturally creep and tend to tighten around the well (Bérest and Brouard, 2003). The gap between fluid pressure and geostatic pressure in the formation at shallow depth (hence, the risk of massive fluid seepage) is larger when product density is smaller. The cemented annular space includes two interfaces: (1) that between the cement and the casing steel; and (2) that between the cement and the rock mass. These interfaces are possible weak points, especially in gas storage caverns, because the steel casing, and the cement in the annulus behind the casing, shrinks and expands alternatively when large pressure swings are applied to the cavern gas; or stretches when creep closure is too large in the roof area. Most often, the cemented part of the well is weaker than the rock formation itself; its tightness is highly sensitive to the quality of the cementing job (Nicot, 2009). Maximum admissible pressure in the cavern is discussed in Section 3.3. The role of the well completion is discussed below.

2.2. Well architecture

The well architecture of four caverns which experienced wellbore leaks is illustrated in Figure 3.

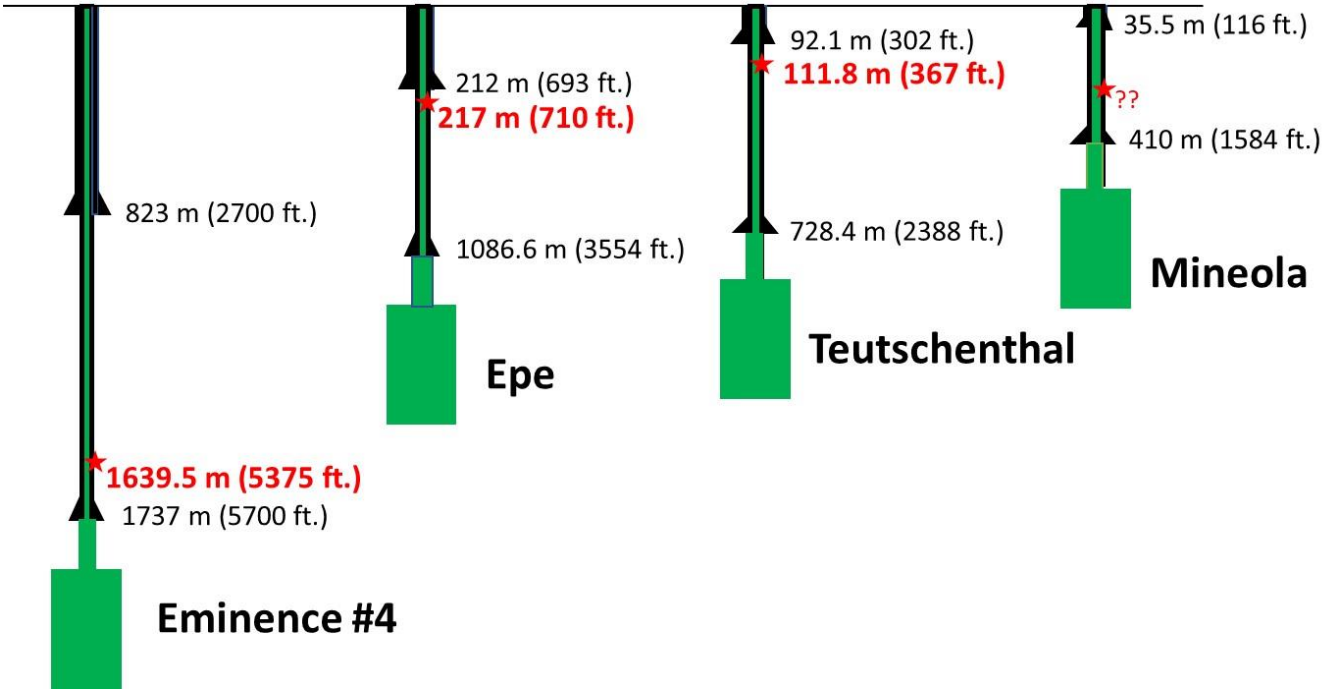

Figure 3. Depths of the two last cemented casings and depth of the breach through the tubing at Eminence, Epe, Teutschenthal and Mineola (Bérest et al., 2019)

The Mineola Storage Terminal is located in the U.S., some 145 km (230 miles) east of Dallas, Texas. The terminal had two storage caverns. One of the wells developed a casing leak. Depths of the two last-cemented casings shoes were 35.5 m and 484 m (115 ft. and 1584 ft) , respectively. Propane escaped through the surface soil to the atmosphere and collected in the low areas around the terminal and surrounding forest. Breach depth was unknown (Gebhardt et al., 2001.)

At Epe, located 90 km (55 miles) north of Dortmund, Germany, S5, a 450,000-m³ (2.7 Mbbls) cavern, had been filled with crude oil since 1980. Depths of the intermediate 16" casing and 11-¾" last-cemented casing shoes were 212 m (693 ft.) and 1086.8 m (3554 ft.), respectively. On February 23 and 24, 2014, a pressure drop of 0.36 MPa (52 psi) was recorded. Video inspection showed a partly unscrewed connection of the 11-¾" casing at a depth of 217 m or 710 ft. (Stöwer, 2018).

The Teutschenthal/Bad Lauchstädt cavern site is located 40 km (25 miles) west of Leipzig, Germany. A pressure drop from 7.5 MPa to 4 MPa (1100 psi to 580 psi) within the ethylene annulus of cavern Ug Lt 5/71 was recorded on March 29 1988. One hour later, the first eruption of ethylene took place. Depths of the intermediate 16-¾" casing and 11-¾" last-cemented casing shoes were 92.1 m (302 ft.) and 728.4 m (2388 ft.), respectively. The surveys performed later showed a damaged connection of the 11-¾" casing at a depth of 111.8 m (Katzung et al.,1996.)

At the Eminence salt dome, located 20 km (12 miles) northwest of Hattiesburg, Mississippi, in the U.S., caverns #1 to #4 were commissioned in the early 1970s. A 28'' hole was drilled to 2700 ft. (823 m), in which a 20''OD cemented casing was set. The last cemented casing shoe, diameter 13-⅜", was at a 5700 ft. (1737-m) depth. On December 26, 2010, a large unexpected pressure drop of 2.5 MPa (3600 psi) in one minute was detected in Cavern #3. Investigations revealed that leakage in that cavern likely arose through salt creep leading to overstretching of the casings above the cavern, where displacements due to creep closure were especially intense (Wellinghoff et al., 2013).

It is interesting to notice that, in most cases, a significant cavern pressure drop was observed although the store products are quite compressible. It means that the leaked products accumulated in an intermediate "receptor" before finding abruptly their way to ground level (Bérest et al., 2019).

2.3. Double barrier

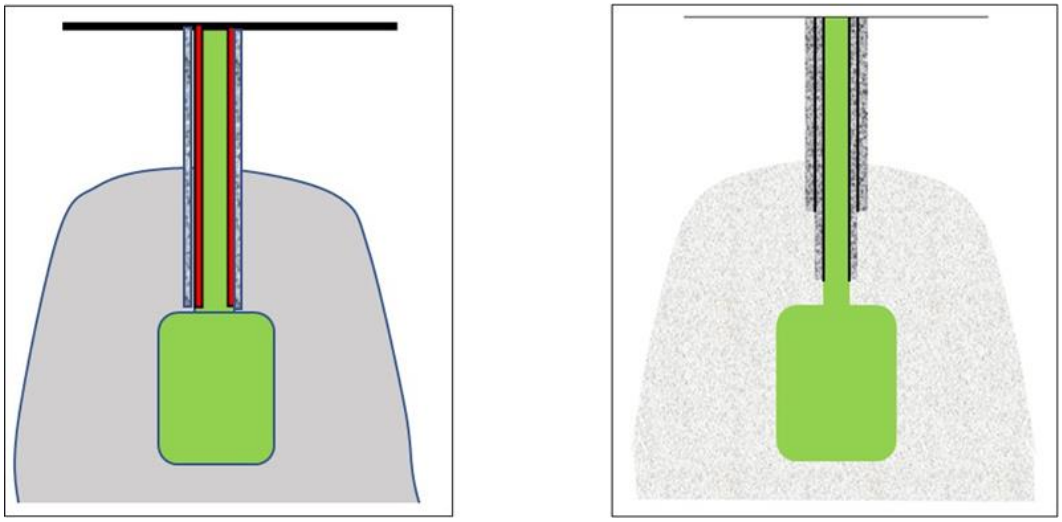

Figure 4 - Schematic completion design: (left) in Europe, a water-filled annulus (in red), isolates the casing from the gas; and (right) in the U.S., the two last-cemented casings are anchored to the salt formation.

In the incidents noted above, and in most casing-failure incidents (Réveillère et al., 2017 – SMRI Report-, Bérest et al., 2019), a breach is created through a steel casing at a depth where the well completion comprises a single cemented casing. In other words, between the shoes of these two casings, a single "barrier" (i.e., a single casing cemented to the rock formation) is present: a breach through the steel casing opens directly to the rock mass. It is interesting to note that, in several cases, when repairing such a leak, an inner steel tube is added to form, with the pre-existing casing, an annular space the bottom of which is closed. This annulus is filled with water whose pressure is monitored at ground level — a way of creating a second "barrier" that did not exist in the initial design. Such a completion (an internal tube delimiting a monitoring annulus closed by a packer at its bottom) is mandatory in France and Germany for natural-gas storage facilities, see Figure 4, left, and the trend in Europe is to equip new liquid-storage caverns with such a system. [It is, for instance, a requirement under Dutch mining law (Koopmans et al., 2014)]. For many years in Texas, Louisiana and Kansas (three states in which can be found the majority of U.S. salt-cavern storages), State regulation has required that new caverns have two cemented casings anchored in the salt formation, see Figure 4, right. In addition, a tightness test is mandatory at least every five years, which covers the case of old caverns that are not equipped with a double casing.

2.4. Lessons learned

It is noticeable that leakage occurrences often happened several dozens of years after well is drilled and cased. This might be the time needed for a breach in the casing to occur through corrosion or for excessive strains in the steel casing to build up through salt creep. In the U.S., to the authors' knowledge, the last incident occurred in Texas in 2005 (where, since 1993, a double casing anchored in the salt formation has been mandatory for new caverns) at Boling, which had only one casing anchored in the salt formation, and in 2001 in Kansas [where similar regulations were enforced in 2003 following the Hutchinson incident, Bérest et al., 2019.] Progressively, the cavern industry adopted more stringent regulations and better testing procedures, which are likely to explain why the number of incidents drastically decreased. The Solution Mining Research Institute, which gathers operators, consultants and academics worldwide, has also contributed to the diffusion of best practices worldwide. In the case of a hydrogen storage cavern, a monitoring annulus is highly recommended, as it is in any gas storage cavern in Germany and France.

3. Selection of the maximum admissible pressure

3.1 Evidence of cavern compressibility increase at high pressure

There are strong indications that overall cavern compressibility increases (a sign of permeability increase) when the pressure gradient at the casing shoe is larger than 0.018-0.019 MPa/m (0.8-0.85 psi/ft.), i.e., 80-85% of the geostatic gradient, which typically is 0.022 MPa/m (1 psi/ft.).

> [Cavern compressibility, or βV, in m^3/MPa, is the ratio between the injected flow rate, Q_{in}, and the concomitant cavern pressure increase, $\dot{P}$, or $Q_{in} = \beta V \times \dot{P}$. An increase of the cavern compressibility is a clear sign of a leak, or Q_{out}, as $\beta V \times \dot{P} = Q_{in} - Q_{out}$ and $\beta_{app} = \beta + Q_{out} / V\dot{P}$.]

A high-pressure test was performed in a brine-filled cavern at Etzel (Germany) in 1990-1992 (Rokahr et al., 2000). It was observed (Figure 5a) that the *apparent* cavern compressibility factor, β, increased significantly, from $\beta = 3.7 \times 10^{-4}$/MPa ($2.55 \times 10^{-6}$/psi) (when the cavern-pressure gradient was 0.019 MPa/m or 0.84 psi/ft)) to $\beta_{app} = 4.7 \times 10^{-4}$/MPa (when it was 0.0205 MPa/m or 0.91 psi/ft.)

Durup (1990, 1994) performed several pressure build-up tests in a wellbore at Etrez (France) in which the pressure was increased through step-by-step brine (or nitrogen) injections. The open-hole length was 198 m (649 ft.). The test lasted six hours. On Figure 4b, the pressure at well-bottom depth (871 m, or 2856 ft.) is plotted against the cumulated injected volume (The slope of this curve is 1/βV). When pressure increased from 14.5 MPa to 20.5 MPa (from 0.017 MPa/m to 0.023 MPa/m at a depth of 871 m), wellbore apparent compressibility increased from $\beta V = 9.7$ liters/MPa (1.15×10^{-5} bbl/psi) to $\beta V = 24$ liters/MPa (2.76×10^{-5} bbl/psi).

This notion was confirmed by Van Heekeren et al. (2009), who measured cavern compressibility as a function of cavern pressure during four pressure build-up tests. Results of these tests are shown on Figure 4c. (No scale is provided in the paper by Van Heekeren et al., 2009.) At low pressure, apparent compressibility is a slowly increasing function of pressure; a pressure threshold can be observed above which apparent compressibility drastically increases. This threshold seems to be significantly smaller than the virgin geostatic pressure. In fact, when successive tests are considered, compressibility is smaller and smaller, and the threshold is higher and higher.

Brückner et al. (2003), described a test performed in a 22-m^3 (132 bbls) cavern leached out at a 448-m depth from a drift at the Bernburg Mine in Germany. In this test, cavern pressure was increased incrementally from zero. At the beginning of the test, 8.8 liters of brine were injected in the cavern: pressure increased by 1 MPa (145 psi), from which it can be inferred that cavern compressibility was $\beta V = 8.8$ liters/MPa ($\beta = 4 \times 10^{-4}$/MPa $= 2.75 \times 10^{-6}$/psi). Cavern compressibility increased over the next steps, becoming $\beta = 4.7 \times 10^{-4}$/MPa when pressure increased from 1.48 MPa to 4.48 MPa (215 psi to 650 psi), a gradient of 4.448/448 = 0.01 MPa/m or 0.44 psi/ft). During the last step, when pressure increased to 9.25 MPa (a gradient of 0.021 MPa/m or 0.93 psi/ft), an "exponential" increase in compressibility was observed.

The origin of such early micro-fracturing, not observed during standard frac tests, is not understood fully. The (macroscopic) state of stresses generated by a swift pressure increase (following a long idle period at low pressure) at the wall of a cavern excavated from a visco-plastic medium (Djakeun-Djizanne et al., 2012) and the (microscopic) state of stresses at the boundaries between salt grains have been implicated.

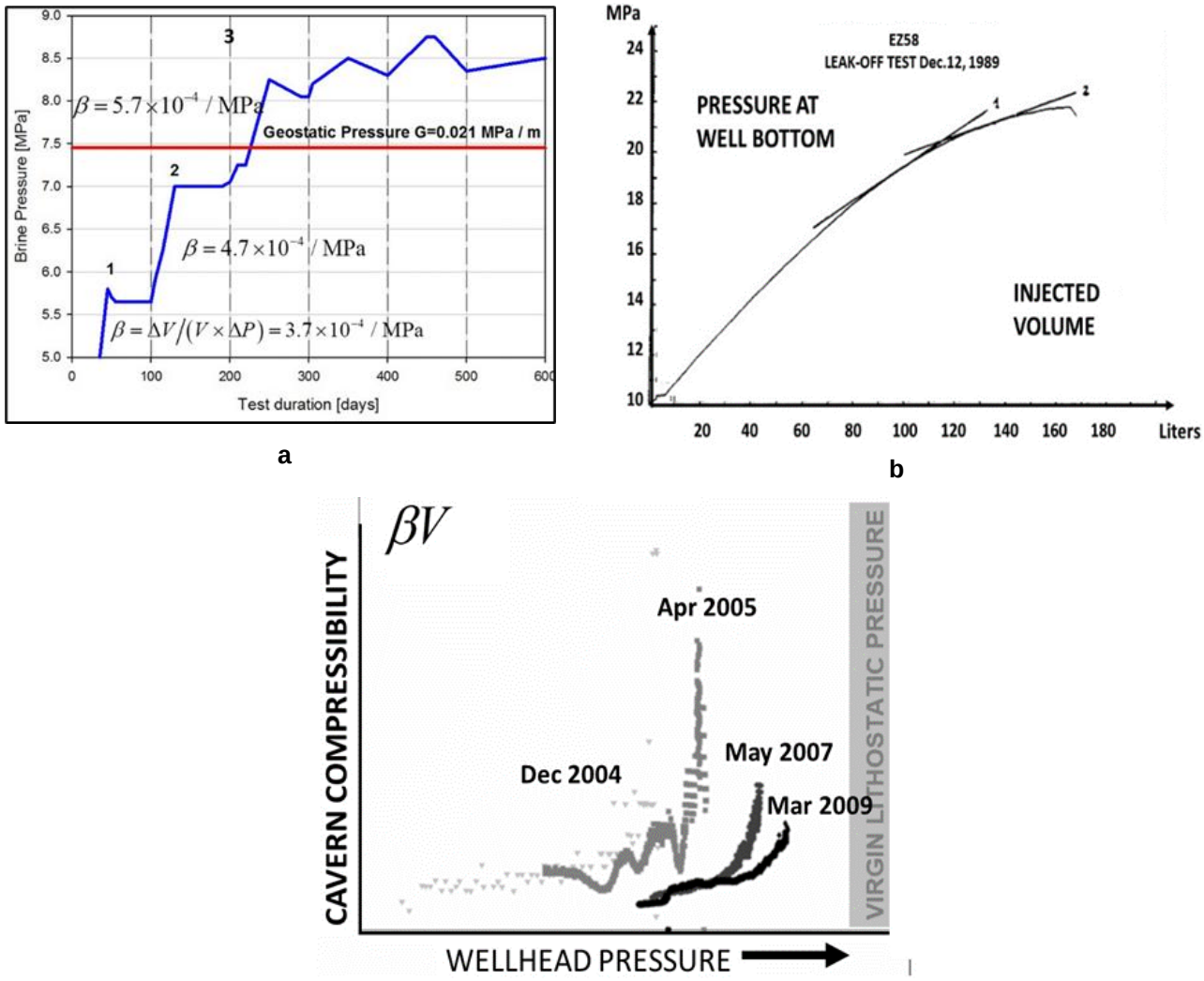

Figure 5 – (a) Etzel test (after Rokahr et al., 2000); (b) Etrez test (after Durup, 1990, 1994); (c) Frisia test (after van Heekeren et al., 2009).

3.2 Maximum pressures in selected gas storage caverns

In Table 1, the maximum gas pressure selected in 24 sites worldwide is represented (Bérest et al., 2020). In most cases, the pressure gradient at casing shoe depth is 0.018 MPa/m (0.8 psi/ft), a value which, although being of empirical origin, is consistent with what was described in Section 3.1.

Table 1 - Maximum pressures in selected gas storage caverns (From Bérest et al., 2020).

Gas storage	Authors	CCS depth (m)	Pmax (MPa)	Maximum gradient (MPa/m)	Maximum gradient (psi/ft)
Aldbrough	Slingsby et al., 2011	1800	27	0.015	0.66
Carriço	Colcombet et al., 2008	1000	18	0.018	0.8
Etzel	Schweinsburg & Schneider, 2010	1150	20	0.017	0.76
Holford	Fawthrope et al., 2013	≈ 550	10	0.018	0.8
Krummhörn	Rummel et al., 1996	≈1500	27	0.018	0.8
Nuttermoor	Bernhardt & Steijn, 2013	≈ 1000	17	0.017	0.76
Teesside	Mullaly, 1982	≈ 350	4.5	0.013	0.58
Zuidwending	Hoelen et al., 2010	1000	18	0.018	0.8

Gas storage	Authors	CCS depth (m)	Pmax (MPa)	Maximum gradient (MPa/m)	Maximum gradient (psi/ft)
Manosque	de Laguérie & Durup, 1994	1000	18	0.018	0.8
Stublach	Pellizzaro et al., 2011	≈ 550	10	0.018	0.8
Egan	Chabannes, 2005	1125	23	0.0204	0.9
Kansas	Itsvan, 1998	NA	12		
China	Fansheng et al., 2010	≈ 2000	17	0.016-0.017	0.72
Aldbrough	McLeod et al., 2011	≈1500	27	0.0155	0.66
Nüttermoor	Bernhardt & Steijn, 2013	≈ 1020	17	0.017	0.8
Germany	Wagler & Draijer, 2013	≈ 648	12.2	0.0188	0.83
Torup	Johansen, 2010			0.0184	0.81
Huai'an	Zhao et al., 2013	1493	26.0	0.0175	0.77
Jintan (Xi-2#)	Yang et al., 2015	937	13.5 15.0	0.144 0.0160	0.64 0.7
Jintan (PetroChina)	Hongling Ma, Institute of Soil and Rock Mechanics, Wuhan, pers.com. (May 2018)	≈1000	17.0 18.0	0.0170 0.0180	0.76 0.8
Jintan (Sinopec)		900	17.0	0.0188	0.83
Qianjiang		1980	32.0	0.0160	0.7

3.3 Maximum pressure in a hydrogen storage

Table 2. Properties of several hydrogen-storage caverns (adapted from Laban, 2020).

	Teesside (UK)	**Clemens Dome (TX)**	**Moss Bluff (TX)**	**Spindletop[a] (TX)**
Type of formation	**Bed**	**Dome**	**Dome**	**Dome**
Operator	**Sabic**	**Chevron Phillips**	**Praxair**	**Air Liquid**
Commissioned	**1972**	**1986**	**2007**	**2014**
Geometrical Volume (m^3)	**210 000**	**580 000**	**566 000**	**906 000**
Mean Cavern Depth (m)	**365**	**1000**	**1200**	**1340 (1150-1400)**
Pressure range (MPa)	**4.5**	**7 - 13.5**	**5.5 – 15.2**	**6.8 – 20.2 [a]**
Pressure gradient (MPa/hm)[b]	**1.2**	**0.7 – 1.35**	**0.46 - 1.27**	**0.6 – 1.76[c]**
Net energy stored (GWh)	**27**	**81**	**123**	**274**
H_2 mass (t)	**810**	**2 400**	**3 690**	**8 230**
Net Volume (std m^3)	**9.12 Mm^3**	**27.3 Mm^3**	**41.5 Mm^3**	**92.6 Mm^3**

[a]From Jallais, 2018 [b]At cavern mid-depth, except for Spindletop [c]At cavern roof depth

Scarce data collected for hydrogen storage caverns has been provided in the literature (Table 2, Jalan, 2020). The Teesside hydrogen storage caverns in the UK are operated according to the brine compensation method; pressure in

the caverns is constant and relatively low. According to Laban (2020), the maximum pressure gradient at mean cavern depth is 0.0135 MPa/m (0.6 psi/ft.) at Clemens Dome in Texas, 0.0127 MPa/m (0.56 psi/ft.) at Moss Bluff and 0.0151 MPa/m (0.67 psi/ft.) at Spindletop. These figures underestimate slightly the gradient at casing-shoe depth (rather than mean depth) – which is the notion generally preferred to compare maximum pressures in different caverns. In addition, Laban (2020) is likely to underestimate the maximum gas pressure at Spindletop which, according to Jallais, 2018, is 20.2 MPa (2930 psi) at a 1340-m (4395 ft.) depth, or a pressure gradient of 0.0173 MPa/m (0.765 psi/ft.) at the cavern-top depth. The reasons for the apparently low gradients at Moss Bluff and Clemens Dome are unknown.

4. Tightness Test (MIT)

4.1. A brief history of tightness tests in salt caverns

The first historical tightness tests (often called Mechanical Integrity Tests' (MITs) in the salt-cavern industry) were of the pressure-vessel (PV) type. Pressure in the brine-filled cavern was increased to the maximum admissible pressure through brine injection (The pressure gradient at the casing shoe depth typically increased from 0.012 MPa/m to 0.018 MPa/m, or 0.52 psi/ft. to 0.8 psi/ft), and further pressure evolution was recorded. A fast pressure decrease was interpreted as the consequence of a significant brine leak. This method is extremely coarse. For instance, Vrakas, 1988, mentions PV tests performed on salt caverns in the U.S. Strategic Petroleum Reserve. During these tests, wellhead pressure *increased,* suggesting a negative leak! In fact, a brine cavern is the seat of many phenomena (other than a leak) that can lead to a severe under- or overestimation of the actual leak. For instance, Brasier, 1990, correctly explained that

The theory […] *is if the salt cavity is "shut in" and a leak develops* […] *a pressure decrease can be observed at the surface. This test was deemed inappropriate for two reasons* […] *given the enormous size of* […] *the cavities, a massive leak would have to be present in order to detect any pressure decrease. Any uncalculated pressure changes in the "shut in" cavity due to temperature fluctuations of cavity fluid, further dissolution of salt and salt heaving will interfere with the interpretation of the results making the test unreliable*. (p. 6).

A quantitative estimate of these "*uncalculated pressure changes*" can be found in Van Sambeek et al., 2005.

A much more precise testing method appeared in the 1990s. The brine-filled cavern, equipped with a central string, is pressurized to testing level, and a nitrogen column is injected in the annular space to develop a brine-nitrogen interface, located below the last casing shoe and above the cavern roof. Interface depth is tracked using a logging tool once a day during a 2-3 days period. The volumetric gas leak can be computed when multiplying the interface rise (The accuracy is $\delta h = 6"$, or 15 cm, typically) by the cross-sectional area of the chimney at interface depth (or Σ, typically a fraction of a m^2).
Correction can be made to take into account possible T, P changes during the test. Changes in gas mass can be computed accurately. This method is much better than the historical PV method, as it focuses on wellbore tightness (the topic of concern, see Section 2) rather than on the complex behavior of the whole cavern. Because it is based on gas mass balance, it is independent of all the phenomena described by Brasier, 1990, and Van Sambeek et al., 2005, which blur the interpretation of pressure changes in the PV method.

4.2. Interpretation of the Tightness Test

Interpretation of the PV test is straightforward. A cavern, as mentioned in Paragraph 3.1, is a compressible body. Any brine withdrawal (Q_{out}) generates a pressure drop, $Q_{out} = \beta V \times \dot{P}$. The compressibility factor, or β, is the sum of (1) the adiabatic compressibility of brine, $\beta_b = 2.57 \times 10^{-4}$ /MPa or 1.77×10^{-6}/psi [which is related to wave speed in brine (c), $\beta_b \rho_b c^2 = 1$], (2) the compressibility of the cavern (the elastic "box" that contains brine), β_c, and (3) the effect of additional dissolution, β_{diss}. (Salt concentration in brine is a function of pressure.) A typical value is $\beta = \beta_b + \beta_c + \beta_{diss} = 4 - 5 \times 10^{-4}$ /MPa or $3 \times 10^{-6} - 3.7 \times 10^{-6}$/psi larger values are found in "flat" caverns (Bérest et al., 1999). These figures explain why accuracy of the PV tests is poor. In the U.S., it is often accepted that the maximum admissible leak rate (MALR) is 1000 bbls/yr., or 160 m^3/yr. When the cavern volume is $V = 600{,}000$ m^3 $(3.6$ mmbbls), cavern compressibility is $\beta V = 300$ m^3/MPa (13 bbls/psi). When the accuracy of the pressure sensor is $\delta P = 1$ kPa (0.15 psi) the tightness test accuracy (i.e., the Minimum Detectable Leak Rate, or MDLR) during a test lasting $\delta t = 2$-day is $2\beta V \times \delta P / \delta t = 300$ liters/day, or 110 m^3/yr. (660 bbls/yr.) – not much smaller than the MALR.

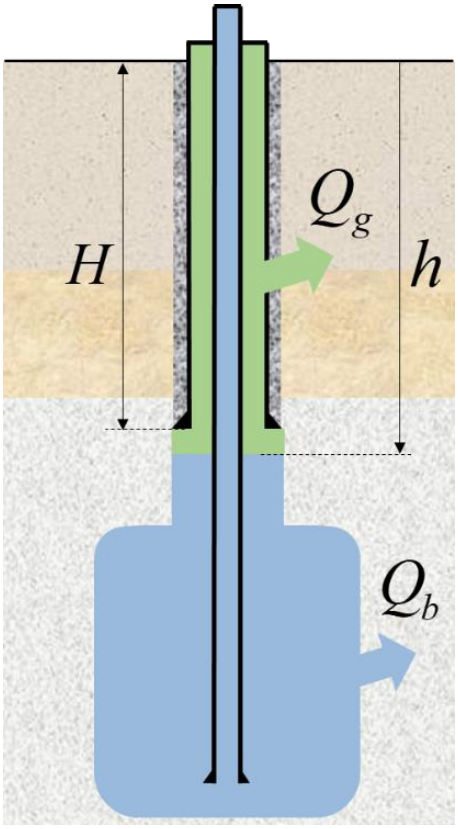

Figure 6. Gas Leak Test (H is the casing-shoe depth; h is the interface depth; Q_g is the gas-leak rate; and Q_b is the brine-leak rate.

The simplest interpretation of the NLT is as follows (Figure 6): the chimney cross-sectional area at interface depth (*h*) is Σ ($\Sigma = 0.03\ \mathrm{m}^2$ is typical), the interface rise rate is $\dot{h} < 0,$ and the gas leak rate is assumed to be $Q_g = -\Sigma \dot{h}.$ Accuracy of the interface tracking tool is $\delta h = 15\ \mathrm{cm}$ (6"). When two consecutive measurements are separated by $\delta t = 3\ \mathrm{days},$ the resolution is $2\Sigma\delta h/\delta t = 3\ \mathrm{liters/day}$ (0.02 bbl/day) — much smaller than the PV resolution. However, this interpretation is a little too simple. It was said that temperature changes in the gas column can be taken into account; however, a ΔT = 0.1 °C temperature change in the gas column during the tests (difficult to detect) generates an uncertainty by $\Delta h = h\,\Delta T/T$ = 0.3 m (12") when interface depth is *h* = 1000 m or 3 300 ft. (Lampe and Ratigan, 2014); in addition, when the interface rises, brine pressure increases accordingly, and the cavern expands, hiding some of the actual leak. More important, using a logging tool is rather expansive and provides information once a day, typically. A continuous method is preferable.

A better interpretation requires modelling. The gas-state equation is $P = \rho r T;$ the three variables are functions of depth (*z*, oriented downward) and

$$\frac{\rho_z'}{\rho} = \frac{P_z'}{P} - \frac{T_z'}{T} = \frac{\rho g}{P} - \frac{G_{geo}}{T} = \frac{1}{T}\left(\frac{g}{r} - G_{geo}\right) \qquad (1)$$

where G_{geo} is the geothermal gradient, and *g* is the gravitational acceleration. For nitrogen, $r_{N2} = 260\ \mathrm{J/kg\text{-}°C},$ $g/r_{N2} = 0.038\ \mathrm{°C/m};$ for hydrogen, $r_{H2} = 4200\ \mathrm{J/kg\text{-}°C}$ and $g/r_{N2} = 0.0023\ \mathrm{°C/m}.$ The average geothermal gradient is $G_{geo}^{av} = 0.02\ \mathrm{°C/m},$ from which, when $T = 300\ \mathrm{K},$ $\rho_z'/\rho = 5\times10^{-5}\ /\mathrm{m}$ for nitrogen, and $6\times10^{-5}\ /\mathrm{m}$ for hydrogen. When the interface depth is $h = 700\ \mathrm{m},$ the relative error made when assuming that density is uniform is 1-2 %. (Obviously, gas density is a function of time.) Gas pressure distribution in the annular space is

$$P_g(z) = P_g^{wh}(t) + \gamma_g(t) z \qquad (2)$$

where $\gamma_g(t) = \rho_g(t) g$ and $P_g^{wh}(t)$ is the wellhead gas pressure. For the brine column in the central string,

$$P_b(z) = P_b^{wh}(t) + \gamma_b z \qquad (2)$$

where $P_b^{wh}(t)$ is the wellhead brine pressure. The gas mass is $m_g = \rho_g(h) V_g$, where V_g is the volume of gas in the annular space above the interface. Its derivative with respect to time equals the gas leak rate:

$$\Sigma \dot{h} + \beta_g V_g \dot{P}_g^{wh} + Q_g = 0 \qquad (4)$$

here $\beta_g = 1/P_g^{wh}$ is the isothermal coefficient of compressibility of nitrogen (It is assumed that thermal equilibrium with the rock mass is reached, as the wellbore diameter is small.) For brine, a similar equation can be found:

$$-\Sigma \dot{h} + \beta V \dot{P}_b^{wh} + Q_b = 0 \qquad (3)$$

where Q_b is the brine leak rate. (In fact, this term includes all the phenomena which, together with the actual brine leak, contribute to brine volume changes, such as thermal expansion.) Finally, gas and brine pressures are equal at interface depth:

$$(1 + \delta_g) \dot{P}_g^{wh} - \dot{P}_s^{wh} + \Delta\gamma \dot{h} = 0 \qquad (4)$$

where $\delta_g = gh/r_g T$ and $\Delta\gamma = \gamma_s - \gamma_g$. Using algebra, these formulas can be written

$$\begin{bmatrix} \beta_g V_g + (1+\delta_g)\Sigma/\Delta\gamma & -\Sigma/\Delta\gamma \\ -(1+\delta_g)\Sigma/\Delta\gamma & \beta V + \Sigma/\Delta\gamma \end{bmatrix} \begin{bmatrix} \dot{P}_g^{wh} \\ \dot{P}_b^{wh} \end{bmatrix} + \begin{bmatrix} Q_g \\ Q_b \end{bmatrix} = \begin{bmatrix} 0 \\ 0 \end{bmatrix} \qquad (5)$$

For hydrogen, in a 1000-m deep cavern, $\delta = gh/r_{H2} T = 0.0073$ (when $T = 320$ K) is very small when compared to 1. (It is less true for nitrogen, $\delta_{N2} = 0.117$; as $r_{N2} = 260$ J/kg/°C instead of $r_{H2} = 4200$ J/kg/°C).

Three "compressibilities" play a role:

(1) cavern compressibility, $\beta V = 20\ \mathrm{m}^3/\mathrm{MPa}$ (0.87 bbl/psi) with cavern volume $V = 50{,}000\ \mathrm{m}^3$ (0.3 mmbls);

(2) compressibility of hydrogen in the annular space $(\beta_g V_g)$ [A simple estimate can be reached as follows. It is assumed that the chimney and the annular space cross-sectional area are not very different — for instance, $\Sigma = 0.024\ \mathrm{m}^2$ (0.258 ft^2) The hydrogen volume is $V_g = \Sigma h$. The pressure gradient at the casing shoe during an MIT typically is $\gamma_t = 0.018$ MPa/m, and $P_g = \gamma_t h = 18$ MPa, from which $\beta_g V_g = \Sigma/\gamma_t = 1.33\ \mathrm{m}^3/\mathrm{MPa}$ (0.0577 bbl/psi); and

(3) interface compressibility, $\Sigma/\Delta\gamma$. When gas temperature and pressure are 300 K and 18 MPa, respectively, the hydrogen density is $\rho_{H2} = P_g/r_{H_2} T = 14\ \mathrm{kg/m}^3$, $\Delta\gamma = \gamma_b - \gamma_{H2} = 0.011$ MPa/m, and $\Sigma/\Delta\gamma = 2.2\ \mathrm{m}^3/\mathrm{MPa}$ (0.0954 bbl/psi);

and the relation between leak rates and wellhead-pressure rates can be written:

$$\begin{bmatrix} 3.53 & -2.2 \\ -2.2 & 22.2 \end{bmatrix} \begin{bmatrix} \dot{P}_g^{wh} \\ \dot{P}_b^{wh} \end{bmatrix} + \begin{bmatrix} Q_g \\ Q_b \end{bmatrix} = \begin{bmatrix} 0 \\ 0 \end{bmatrix} \quad (8)$$

where units are m^3/day and MPa/day (or liters/day and kPa/day). Two lessons can be drawn from these formulas.

1. The simplest interpretation of the NLT-type test, $(Q_g = -\Sigma\dot{h})$, can be wrong. When the gas leak rate is zero, the gas-brine interface can move when a brine leak is present, $Q_s - \left(1 + \beta V / \beta_b V_g + \beta V \Delta\gamma / \Sigma\right)\Sigma\dot{h} = 0$, giving the illusion of a "negative" leak, or $Q_g < 0$.
2. The gas-leak can be inferred from wellhead pressure evolutions. In the example discussed above, $Q_g\left[\text{L/day}\right] = 3.53\,\dot{P}_g^{wh}[\text{kPa/day}] - 2.2\dot{P}_b^{wh}[\text{kPa/day}]$. A good accuracy value is reached when the minimum detectable flow rate is much smaller than the maximum admissible leak rate, which is 500 liters/day (3 bbls/day).. This condition is met when the accuracy of the pressure gages is 1 kPa (1.5 psi).

This is important, as tracking the brine-gas interface with a logging tool is expensive. In the following, we suggest performing several tightness tests, with the interface being at several depths in the borehole (Figure 6). The method presented here allows continuous measurement of the leak rate at a low cost.

4.3. Fail/Pass criteria

Two methods can be used to assess tightness test results. The first method, used widely in the nuclear industry, consists of building a safety case. A safety case includes seepage scenarios and consequences, variants, worst cases, computations and statistical analyses. Such a method is not used in the underground storage industry, as the occurrence of leak paths below ground are practically unpredictable (as suggested by Section 2), leading to unrealistic scenarios. The second method is more empirical; it is based on experience, analysis of past incidents and accidents, and collection of data on good practices in the industry.

The first fail/pass criteria for tightness tests were discussed by Van Fossan, 1983, and by Van Fossan and Whelply, 1985. These researchers introduced a fundamental distinction between the Minimum Detectable Leak Rate (MDLR), or test resolution, which results from analysis of the various uncertainties of the testing method, and the Maximum Admissible Leak Rate (MALR), which results from *a priori* economic and safety considerations. (This was a considerable breakthrough; at that time, it often was considered sufficient that the as-measured leak rate be smaller than the MDLR —not a big incentive to thorough tracking of uncertainties.) In 1995 Crotogino, in a report for the Solution Mining Research Institute, suggested that, for a Nitrogen Leak Test, the MDLR and the MALR be 50 kg/day (110 lbs/day) and 150 kg/day (330 lbs/day), respectively. (When it is assumed that, at cavern-shoe depth, pressure and temperature are 17 MPa (2 465 psi) and 300 K, respectively, 150 kg/day is equivalent to 0.8 m^3/day, or 300 m^3/yr). In the U.S., 1000 bbls/yr (160 m^3/yr) is somewhat of a standard for the MALR. (The value of 160 m^3/yr in a 320,000-m^3 cavern means that the relative leak rate is 5×10^{-4}/yr, a remarkable achievement.)

Crotogino's figures apply to a Nitrogen Test; for other fluids, he suggests taking fluid viscosity into account. Hydrogen is 15 times lighter than nitrogen and its viscosity is twice as low as that for nitrogen. Schlichtenmayer and Bannach, 2015, measured salt permeability to nitrogen, hydrogen and natural gas at the laboratory and concluded that "*The main result of the measurements is that practically no difference in the permeability of rock salt for natural gas, hydrogen and air could be observed. Any difference in the permeation rates of the gases through a portion of rock salt (given that there are permeation paths existing) results only from their different viscosities*" (p. iv). It is noted that this might not be true for the steel casings.

An MALR of 50 kg/day or 110 lbs (three times smaller than the leakage flowrate in kg/day, five times larger than the leakage flow rate in m^3/day suggested by Crotogino for nitrogen) can be considered as a provisional initial reference, open to discussion, and to be revised when additional experience (from tightness tests) becomes available.

4.4. Tightness Tests in a hydrogen salt cavern

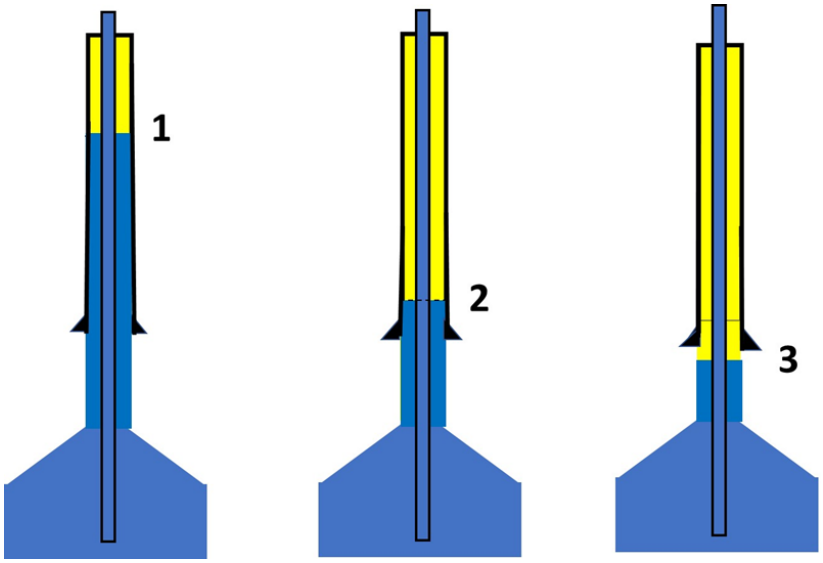

Figure 7. Different interface depths during the tests with gas.

Several hydrogen storage facilities in salt caverns are planned to be created and operated in Europe. They will be the firsts of their kind (except for “compensated” caverns in Teesside, UK, commissioned in the 1970s). Hydrogen is a mobile gas, and the consequences of a leak reaching ground level might be severe. For these reasons, checking tightness is especially important, as adhesion to such projects by the regulatory authorities and the public is required. It is suggested that, at least for the first hydrogen caverns to be created, four tightness tests be performed, as described below.

- After drilling, a PV test (leak-off test) of the brin-filled borehole is performed. Brine pressure during the test is the maximum admissible pressure during operation. This test lasts for a few days.
- Before commissioning, an NLT test is performed (Figure 7). Monitoring wellhead pressures and interface tracking with a logging tool are used to interpret the tests. The gas-brine interface in the annular space is set at different depths, successively: at borehole mid-depth (to check the accuracy of the measurement system through small deliberate gas withdrawal); above the casing shoe; and below the casing shoe (to identify possible leak locations).
- The same test is repeated with hydrogen.
- Tightness of the water-filled annular space is tested.

5. Conclusions

Several cases of tightness loss in gas storage caverns were described. They originate in a weakness of the salt formation (Anomalous Zone) or in the presence of a single casing between the stored gas and the rock formation (Single Barrier). The maximum gas pressure must be lower than 80-85 % of the geostatic pressure at the casing-shoe depth. It is recommended to have two barriers between the rock mass and the salt formation (according to the current practice, two

cemented casings in North America, and one cemented casing and one water-filled annular space in Europe). Tightness tests must be performed both before leaching the cavern and before the first gas fill. The well is tested with nitrogen and hydrogen, successively. During these tests, the gas-brine interface is set at three distinct depths to assess the tightness of the various parts of the wells. For computing the leak rate during the test, in addition to interface tracking, a continuous and non-intrusive method is suggested.

Acknowledgements

The study presented in this paper was funded partly by the French program *Investissements d'Avenir*, managed by Géodénergies in support of the Stopil-H2 Project, devoted to the feasibility study of a pilot storage of H_2 in a salt cavern. This project includes researchers from Air Liquid, Armines (Mines ParisTech and Ecole Polytechnique), BRGM, Brouard Consulting, Geostock, Ineris and Storengy. It also received funding from the Fuel Cells and Hydrogen 2 Joint Undertaking under grant agreement No 101006751. This Joint Undertaking receives support from the European Union's Horizon 2020 research and innovation programme and Hydrogen Europe and Hydrogen Europe Research.

References

Bauer S.J., Ehgartner B.L., Neal J.T. (2000) Geotechnical Studies Associated with Decommissioning the Strategic Petroleum Reserve Facility at Weeks Island, Louisiana: A Case History, in: *Proc. Technical Class and Technical Session SMRI Fall Meeting*, San Antonio, 146-156.

Bérest P., Brouard B. (2003) Safety of salt caverns used for underground storage, *Oil & Gas Sci. and Tech. Rev. Ifpen*, **58**, 3:361-384.Bérest P., Bergues J., Brouard B. (1999) Review of static and dynamic compressibility issues relating to deep underground salt caverns*, Int. J. Rock Mech. Min. Sci.,* **36**, 1031-1049.

Bérest P., Brouard B., Karimi-Jafari M., Réveillère A. (2020) Maximum admissible pressure in salt caverns used for brine production and hydrocarbon storage, *Oil & Gas Sci. and Tech. Rev. Ifpen*, ogst.ifpenergiesnouvelles.fr https://doi.org/10.2516/ogst/2020068.

Bérest P., Réveillère A., Evans D., Stöwer M. (2018) Review and analysis of historical leakages from storage salt caverns wells, *Oil & Gas Sci. and Tech. Rev. Ifpen*, DOI: 10.2516/ogst/2018093.

Brasier FM. (1990) Assuring the integrity of solution mining operations, in: *Proc. SMRI Fall Meeting, Paris, France.*

Brückner D., Lindert A., Wiedemann M. (2003) The Bernburg Test Cavern —A Model Study of Cavern Abandonment, in: *Proc. SMRI Fall Meeting, UK.*

Carosella M.E. (1978) The Use of Salt Domes for the Strategic Petroleum Reserve, in: *Proc. 5th Symp. on Salt,* A.H. Coogan and L. Hauber ed., Northern Ohio Geological Society Inc. Pub., Vol. II, p. 69-75.

Cartwright M.J., Ratigan J.L. (2005) Case History —Solution Mining a Cavern That Intersects a Plane of Preferred Dissolution, in: *Proc. SMRI Fall Meeting, Nancy, France.*

Crotogino F. (1995) *External well mechanical integrity testing/performance, data evaluation and assessment*, SMRI Research Project, Report no. 95-0001-S. www.solutionmining.

Djakeun-Djizanne H., Berest P., Brouard B. (2012) Tensile effective stresses in hydrocarbon storage caverns**,** in: *Proc. SMRI Fall Meeting, Bremen, Germany.*

Durup J.G. (1990*) Long term tests for tightness evaluations with brine and gas in salt (Field test n°1 with brine),* Research Project Report n°90-2-SMRI. www.solutionmining.Durup JG. (1994) Long term tests for tightness evaluations with brine and gas in salt, in: *Proc. SMRI Fall Meeting, Hannover, Germany.*

Fokker P.A., In't Veld C., Bakker T.W., Jagt M. (2004) 10 years' experience in squeeze mining, in: *Proc. SMRI Fall Meeting, Berlin, Germany.*

Gebhardt F., Eby D., Barnett D. (2001) Utilizing Coiled Tubing Technology to Control a Liquid Propane Storage Well Fire, A Case History, in: *Proc. SMRI Spring Meeting, Orlando, Florida.*

Hoffman E.L., Ehgartner B.L. (1997) Using Three Dimensional Structural Simulations to Study the Interactions of Multiple Excavations in Salt, *SAND 97-1017C Report*, Sandia National Laboratories, Albuquerque, N.M.

Jallais S. (2018) Enjeux du stockage et vecteurs fluides énergétiques, oral presentation at Paris Innovation Campus https://www.geosciences.minesparis.psl.eu/wp-content/uploads/2020/01/MESSAGES_progr5-SJallais.pdf

Johnson D.O. (2003) Regulatory response to unanticipated geo-mechanical events effecting gas storage cavern operations in Texas, in: *Proc. SMRI Spring Meeting, Houston, Texas.*

Katzung G., Krull P., Kühn F. (1996) Die Havarie der UGS Sonde Lauchstädt 5 im Jahre 1988, Auswirkungen und geologische Bedingungen, *Zeitschrift für Angewandte Geologie*, 42, 1, 19 – 26 (in German).

Kirmic A., Rałowicz B. (2003) The selected cases of surveying salt caverns geometry in Turquish Arabali Field made by Echosonda-Chemkop, in: *Proc. SMRI Fall Meeting, Chester, UK.*

Koopmans T., Groenenberg R., Pinkse T. (2014) 21st century gasoil storage in Twente, The Netherlands. State-of-the art, multiple-barrier design based on a novel risk management approach, in: *Proc. SMRI Fall Meeting, Groningen, The Netherlands.*

Kupfer D.H. (1990) Anomalous Features in the Five Islands Salt Stocks, Louisiana, *Trans. Gulf Coast Assoc. Geo. Soc.,* v. XL: 425-437.

Laban M.P. (2020) Hydrogen storage in salt caverns. Chemical modelling and analysis of large-scale hydrogen storage in underground salt caverns. Mast. Sci., Delft University of Technology, 86 p.

Lampe B., Ratigan J.L. (2014) Pitfalls of a Nitrogen-Brine interface Mechanical Integrity Test, in: Proc. SMRI Spring Meeting, San Antonio, 19-30.

Looff K. (2017) The Impact of Anomalous Salt and Boundary Shear Zones on Salt Cavern Geometry, Cavern Operations, and Cavern Integrity, in: *Proc. SMRI Spring Meeting, Albuquerque, New Mexico.*

McCauley T.V., Ratigan J.L., Sydansk R.D., Wilson S.D. (1998) Characterization of the Brine Loss Zone and Development of a Polymer Gel Plugging Agent to Repair Louisiana Offshore Oil Port (LOOP) Cavern 14, in: *Proc. SMRI Fall Meeting, Roma, Italy.*

Nicot JP. (2009) A survey of oil and gas wells in the Texas Gulf Coast, U.S.A., and implications for geological sequestration of CO2, *Environ. Geol.,* **57,**1625 – 1638.

Réveillère A., Bérest P., Evans DJR., Stöwer M., Bolt R., Chabannes C., Koopmans T. (2017) *Past salt caverns incidents database Part 1: Leakage, Overfilling and Blow-out,* SMRI Research Report RR2017-2. 124p. www.solutionmining.

Rokahr R.B., Hauck R., Staudtmeister K., Zander-Schiebenhöfer D.Z. (2000) The results of the pressure Build-up test in the brine filled cavern Etzel K102, in: Proc. SMRI Fall Meeting, San Antonio, Texas.

Schlichtenmayer M., Bannach A. (2015) *Renewable Energy Storage in Salt Caverns- A Comparison of Thermodynamics and Permeability between Natural Gas, Air and Hydrogen*, SMRI Research Report RR2015-01. www.solutionmining.

Smit A.J. (2019) Sudden pressure drop in Nedmag cavern cluster, in: *Proc. SMRI Fall Meeting, Berlin, Germany.*

Stöwer (2018), in: Réveillère et al., (2018).

Thoms R.L., Neal J.T. (1992) Effects of anomalous features on solution mining of storage caverns in domal salt, in: *Proc. SMRI Fall Meeting, Houston, Texas*.

Van Fossan N.E. (1983) The characterization of mechanical integrity for cased boreholes entering solution caverns, in: *Proc. 6th Int. Symp. on Salt, Vol. II: The Salt Institute*; 111-120.

Van Fossan N.E., Whelply F.V. (1985) Nitrogen as a testing medium for proving the mechanical integrity of wells, in: *Proc. SMRI Fall Meeting, Houston.*

Van Heekeren H., Bakker T., Duquesnoy T., de Ruiter V., Mulder L. (2009) Abandonment of an extremely deep cavern at Frisia Salt, in: *Proc. SMRI Fall Meeting, Krakow, Poland.*

Van Sambeek L.L., Bérest P., Brouard B. (2005) *Improvements in Mechanical Integrity Tests for solution-mined caverns used for mineral production or liquid-product storage*, SMRI Research Project Report 2005-1, 142 p.

Vrakas J. (1988) Cavern integrity testing on the SPR program, in: *Proc. SMRI Spring Meeting, Mobile, Alabama.*

Wellinghoff J., Moeller P.D., Norris J.R., LaFleur C.A., Clark T.T. (2013) Order approving abandonment, amending certificate authority, and granting clarification, United States of America Federal Energy Regulatory Commission (FERC) decision relating to Transcontinental Gas Pipe Line Company.